Original Article

Granulomas Following Subcutaneous Injection With Aluminum Adjuvant-Containing Products in Sheep

Veterinary Pathology
1-11

DOI: 10.1177/0300985818809142
journals.sagepub.com/home/vet

Javier Asín[1], Jéssica Molín[1], Marta Pérez[2], Pedro Pinczowski[1], Marina Gimeno[1], Nuria Navascués[3], Ana Muniesa[1], Ignacio de Blas[1], Delia Lacasta[1], Antonio Fernández[1], Lorena de Pablo[4], Matthew Mold[5], Christopher Exley[5], Damián de Andrés[4], Ramsés Reina[4], and Lluís Luján[1]

Abstract

The use of vaccines including aluminum (Al)–based adjuvants is widespread among small ruminants and other animals. They are associated with the appearance of transient injection site nodules corresponding to granulomas. This study aims to characterize the morphology of these granulomas, to understand the role of the Al adjuvant in their genesis, and to establish the presence of the metal in regional lymph nodes. A total of 84 male neutered lambs were selected and divided into 3 treatment groups of 28 animals each: (1) vaccine (containing Al-based adjuvant), (2) adjuvant-only, and (3) control. A total of 19 subcutaneous injections were performed in a time frame of 15 months. Granulomas and regional lymph nodes were evaluated by clinicopathological means. All of the vaccine and 92.3% of the adjuvant-only lambs presented injection-site granulomas; the granulomas were more numerous in the group administered the vaccine. Bacterial culture in granulomas was always negative. Histologically, granulomas in the vaccine group presented a higher degree of severity. Al was specifically identified by lumogallion staining in granulomas and lymph nodes. Al median content was significantly higher ($P < .001$) in the lymph nodes of the vaccine group (82.65 μg/g) compared with both adjuvant-only (2.53 μg/g) and control groups (0.96 μg/g). Scanning transmission electron microscopy demonstrated aggregates of Al within macrophages in vaccine and adjuvant-only groups. In these two groups, Al-based adjuvants induce persistent, sterile, subcutaneous granulomas with macrophage-driven translocation of Al to regional lymph nodes. Local translocation of Al may induce further accumulation in distant tissues and be related to the appearance of systemic signs.

Keywords

aluminum-based adjuvants, granuloma, macrophage, sheep, lymph node, vaccine

Sheep production in Spain very frequently involves vaccination for prevention of a variety of diseases[25] using vaccines that include aluminum (Al)–based adjuvant. Vaccines are injected throughout the life of the animals, and often a single sheep can receive 2 to 4 vaccines per year or more depending on the specific health problems of a certain flock or the implementation of compulsory vaccination campaigns against emerging infections.[7] The repetitive injection of Al-containing vaccines in sheep has been related to a systemic, previously unreported syndrome, the so-called ovine autoimmune/inflammatory syndrome induced by adjuvants (ovine ASIA syndrome). This was widely observed following the compulsory bluetongue vaccination campaign at the end of the past decade, which resulted in severe deleterious effects on local sheep production.[12,27,36] To date, ovine ASIA syndrome is consistently observed in field

[1]Department of Animal Pathology, University of Zaragoza, Zaragoza, Spain
[2]Department of Animal Anatomy, Embryology and Genetics, University of Zaragoza, Zaragoza, Spain
[3]Institute of Nanoscience of Aragón (INA), University of Zaragoza, Zaragoza, Spain
[4]Institute of Agrobiotechnology, CSIC–Public University of Navarra, Government of Navarra, Navarra, Spain
[5]Lennard-Jones Laboratories, The Birchall Centre, Keele University, Staffordshire, UK

Supplemental material for this article is available on the *Veterinary Pathology* website at http://journals.sagepub.com/doi/suppl/10.1177/0300985818809142.

Corresponding Author:
Lluís Luján, Department of Animal Pathology, Veterinary Faculty, University of Zaragoza, 177 Miguel Servet Street, 50013 Zaragoza, Spain.
Email: Lluis.Lujan@unizar.es

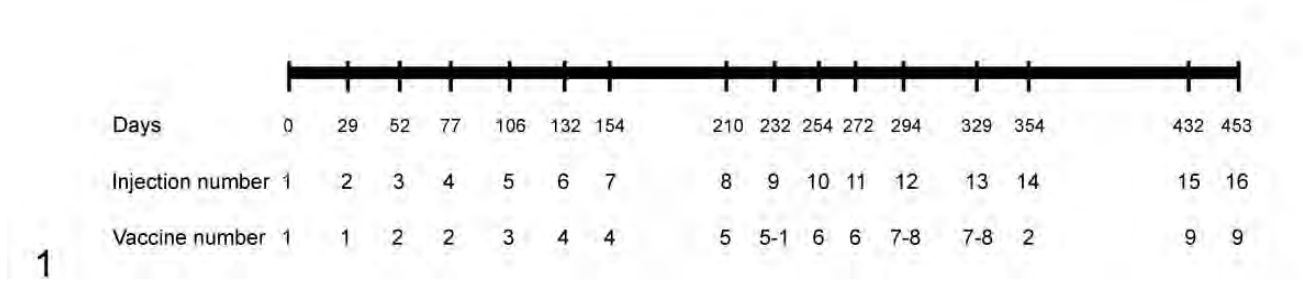

Figure 1. Vaccination schedule for this experiment. The number of days after the first injection is shown. Injection number is the sequential number of a given injection. Vaccine number refers to the vaccine products as described in Suppl. Table S2.

conditions, and there is an urgent need to understand its pathogenesis to control its effects.

Al salts are effective adjuvants that promote a robust immune response against vaccine antigens and are considered safe.[1,26] Some studies indicate these compounds activate the inflammasome pathway, induce a Th2 immune response, and promote specific humoral immunity.[1,9] In veterinary medicine, granulomas associated with Al adjuvants are considered an acceptable side effect,[37] although the use of Al as adjuvant can be related to a broad spectrum of local reactions at the injection site, including chronic severe inflammation leading to sarcomas in cats.[3,16,17] Sheep are considered prone to the development of vaccine-associated granulomas[37,40] and preclinical safety studies for sheep vaccine development usually include periodical in vivo evaluation of the reactions at the injection site over a period of a few months.[2,33]

There are no reported histologic descriptions of the acute or subacute inflammatory response to vaccines.[15] Moreover, a complete pathologic characterization of vaccine-induced granulomas in sheep, including location of Al within granulomas and lymph nodes, has never been performed. This work aims to characterize granulomas induced by vaccines that include an Al-based adjuvant and to establish if Al is transported from the injection site to the regional lymph node.

Materials and Methods

Study Design

The Ethical Committee of the University of Zaragoza approved and licensed all experimental procedures (ref. PI15/14). Requirements of the Spanish Policy for Animal Protection (RED53/2013) and the European Union Directive 2010/63 on the protection of experimental animals were always fulfilled.

The study was based on 4 flocks of 21, three-month-old, neutered male lambs ($N = 84$). Flock 1 was established at the experimental farm of the University of Zaragoza and included purebred Rasa Aragonesa lambs selected from a pedigree flock of certified good health. This flock was always maintained indoors, with optimal conditions of housing, management, and diet. The animals that made up flocks 2 to 4 were selected from 3 commercial flocks representing different management conditions and geographical areas (Suppl. Table S1). Flocks 2 to 4 were maintained within the original commercial flock for the whole experiment. Each flock of 21 lambs was divided into 3 treatment groups (vaccine, adjuvant-only, and control; $n = 7$ each). For the purpose of the present work, these 3 groups included all animals under the same treatment ($n = 28$ each). Two animals from each treatment group died for unrelated reasons during the course of the experiment; therefore, each group consisted of 26 animals at the end of the experiment. The complete study lasted 15 months, from February 2015 to April 2016.

Lambs underwent an accelerated vaccination schedule, receiving, within an acceptable experimental time frame, an Al load equivalent to 6 to 7 years in the field.[25,27] Animals in each treatment group received a total of 19 subcutaneous injections at 16 injection dates, as there were 3 days that required double injections (Fig. 1). Periods between injections ranged from 18 to 78 days (mean = 30.2 $\pm$ 16.0 days). All injections were performed in the subcutaneous tissue of the area encompassing scapula and ribs. Sixteen injections were performed in the right flank, and those 3 corresponding to double injection dates were performed in the left flank. For the purpose of this study, only the 16 injections in the right flank were considered.

The vaccine group was inoculated with commercial vaccines against major ovine diseases (Suppl. Table S2). The recommended period between vaccines and the application procedure for each product was always fulfilled. The adjuvant-only group was injected with Alhydrogel ®(CZ Veterinaria, Pontevedra, Spain), the Al-based adjuvant used in the vaccine preparations. The concentration of Al for each inoculum was calculated to be identical to that of the corresponding vaccine by dilution with phosphate-buffered saline (PBS). The Al content in the adjuvant and each vaccine was established by inductively coupled plasma atomic emission spectrometry (Suppl. Table S2). Vaccine and adjuvant-only groups received a total of 81.29 mg of Al per animal. The control group was inoculated with the same volume of PBS only. All animals received the last injection 5 days prior to euthanasia.

In Vivo Studies

At each injection date, the same evaluator (J.A.) assessed by palpation the severity of reaction to the injections. A range of

degree of severity was established (0–3): 0, no reaction, 1, 1 nodule-forming reaction smaller than 0.5 cm; 2, 1 nodule-forming reaction bigger than 0.5 cm; 3, 1 nodule with central liquefaction and/or fistulation or more than 1 palpable nodule-forming reaction. This assessment was carried out up to and including the 14th injection (Fig. 1).

Pathologic Characterization

A complete necropsy including a systematic sampling of all tissues was performed, but for the purpose of this work, only features recorded in the right flank or in the right prescapular lymph node will be described. This sample collection procedure guaranteed the required samples for the study (see below) since the number of injections was higher in the right flank, and helped in collecting the samples in a minimal time frame. The subcutaneous tissue was exposed and the adipose panniculus dissected. All grossly visible injection nodules were recovered and their number recorded. The presence of central necrosis within the nodules was also recorded. Depending on the number of nodules found in each animal, four categories were established: 0, 1–2, 3–7, and 8 or more nodules.

For histopathologic purposes, only chronic, well-developed nodules were considered, avoiding acute tissue reactions corresponding to the injections performed 5 days before euthanasia. Nodules were fixed and embedded in paraffin, but only 1 per animal was randomly selected for detailed histopathologic studies. This procedure was based on the very homogeneous histopathologic characteristics of nodules (see the Results section). Samples were also obtained from the regional (right prescapular) lymph node. In total, 47 injection-site nodules (24 from the vaccine and 23 from the adjuvant-only animals), 26 control injection site areas, and 76 lymph nodes (26 from the vaccine, 24 from adjuvant-only, and 26 from control animals) were analyzed. Tissues were routinely processed and stained with hematoxylin-eosin. The semiquantitative histopathologic scoring system of the injection-site nodules and prescapular lymph nodes is detailed in Supplemental Table S3 and Supplemental Table S4. Two authors (J.A. and L.L.) performed a blind and individual microscopic evaluation of these parameters, reaching a final consensus.

Microbiology

A total of 40 animals (flocks 1 and 4) were studied by microbiological means: Twenty-six injection site nodules (13 from the vaccine and 13 from the adjuvant-only groups), together with 14 areas of injection from control animals, were submitted for routine microbiologic studies. Each sample was studied by direct Gram staining in smears and incubation of microbiologic cultures in aerobic conditions (Columbia blood agar and MacConkey agar; Oxoid, Basingstoke, Hampshire, UK; up to 48 hours at 37°C) and anaerobic conditions (Columbia blood agar, up to 5 days at 37°C). Basic phenotypic bacterial identification was based on colony and cell (Gram stain) morphology and by standard biochemical tests.

Aluminum In Situ Studies

The presence of Al in granulomas and lymph nodes was studied by fluorescence microscopy with lumogallion staining and by electron microscopy. For fluorescence microscopy, 4 randomly selected injection site nodules from animals in flock 1 (2 from the vaccine and 2 from the adjuvant-only groups) were studied, along with two injection-site areas from control lambs. Samples from the corresponding right prescapular lymph nodes of the same six above-mentioned animals were also analyzed. A protocol to identify Al in tissue sections using lumogallion staining was followed.[30,31] Briefly, 5-μm tissue sections were dewaxed, rehydrated, and incubated with a 1-mM solution of lumogallion (Tokyo Chemical Industry, UK) prepared in 50 mM PIPES rinse solution. Serial control sections were in PIPES rinse solution only. Slides were washed 6 times with PIPES, rinsed in ultrapure water, and mounted with an aqueous medium. Lumogallion and control autofluorescence analyses were performed using a bandpass excitation filter of 470 to 495 nm.

Eight randomly selected injection site nodules from flock 1 (4 from vaccine and 4 from adjuvant-only animals, including those animals analyzed by fluorescence microscopy) were submitted to scanning transmission electron microscopy (STEM) and energy-dispersive X-ray spectroscopy (EDS). Briefly, selected tissues were fixed in 2.5% glutaraldehyde plus 2% paraformaldehyde (0.1 M PBS) washed in PBS, post-fixed in 2% osmium, dehydrated in increasingly graded acetone, and embedded in araldite. Selected ultra-thin sections were counterstained with 1% uranyl acetate and Reynold's lead citrate. STEM images were obtained in a Tecnai F30 microscope (FEI Company, Hillsboro, OR, USA) equipped with an EDS detector. Al determinations by EDS were always performed in intracytoplasmic aggregates, whereas determinations in nuclei were used as internal negative controls. Al particle size and Al aggregates area were measured using STEM images: the length of Al particles was determined in 4 STEM images per animal at 68 000× magnification by measuring 10 particles per image (40 particles per animal), and the area of Al aggregates was established in 4 STEM images per animal at 8500× by measuring 5 well-delimited aggregates per image (20 aggregates per animal). Large, dense eosinophilic crystalloid bodies (made up of Al, see description below; Suppl. Table S3) were not included in the calculation of the area occupied by Al aggregates.

Aluminum Content in Lymph Nodes

Twelve lymph nodes (4 from each group, including the animals analyzed by fluorescence microscopy, STEM, and EDS) were analyzed by microwave digestion followed by transversely heated graphite furnace atomic absorption spectroscopy (TH GFAAS).[19] Briefly, 3 replicate portions of 0.3 to 0.5 g from each lymph node were dried in a 37°C incubator until reaching a constant weight. They were then digested in a microwave (MARS Xpress CEM Microwave Technology Ltd.) in a

Figures 2–7. Injection site granulomas, subcutaneous tissue of the right flank (fat has been removed), lambs injected subcutaneously with vaccine or adjuvant-only. **Figure 2.** Vaccine group. Multiple well-defined granulomas are observed. **Figure 3.** Vaccine group. Thirteen subcutaneous granulomas isolated from a single animal. Nodules used for microbiology and electron microscopy are not present. **Figure 4.** Vaccine group. Well-defined, round, and prominent granuloma. **Figure 5.** Adjuvant-only group. Ill-defined, flat, and inconspicuous granuloma. **Figures 6–7.** Cut section of granulomas. **Figure 6.** Vaccine group. Massive central sterile caseous necrosis. **Figure 7.** Adjuvant-only group. Homogeneous and solid aspect, with no apparent necrosis.

mixture of 1 mL 15.8 M HNO_3 and 1 mL of 30% *w/v* H_2O_2. Upon cooling, each digest was diluted to 5 mL with ultrapure water, and total Al was measured using an atomic absorption spectrometer with a transversely heated graphite atomizer, longitudinal Zeeman-effect background corrector, and an AS-800 autosampler with WinLab32 software (PerkinElmer, Buckinghamshire UK). The Zeeman background corrected peak area of the atomic absorption signal was used for determinations. Results were expressed as micrograms of Al per gram of tissue dry weight. Each determination was the

Table 1. Number (%) of Granulomas Collected Postmortem in Lambs Injected With Phosphate-Buffered Saline (Control), Adjuvant-Only or Vaccines ($n = 26$ Animals per Group).[a]

	No. of Granulomas			
Group	0	1–2	3–7	≥8
Control	26 (100.0)	0 (0.0)	0 (0.0)	0 (0.0)
Adjuvant	2 (7.7)	14 (53.9)	7 (26.9)	3 (11.5)
Vaccine	0 (0.0)	0 (0.0)	6 (23.1)	20 (76.9)

[a] Association was assessed using likelihood ratio ($P < .001$).

arithmetic mean of 3 injections, with a relative standard deviation of 10%.

Statistical Analysis

Qualitative variables, as groups of treatment and histopathologic features, were described using absolute and relative frequencies. Assessment of the associations between 2 qualitative variables was carried out using Pearson's chi-square test (or, alternatively, likelihood ratio for $n \times m$ tables or Fisher's exact test for 2×2 tables).[5]

Shapiro-Wilk test was used to check if the data of the quantitative variables (severity of the in vivo reactions, Al particle length/aggregates, and Al content) followed a normal distribution. As all of them were not normal, they were described using median and interquartile range (IQR) and graphically represented using box and whiskers plots. Association of a nonnormal quantitative variable with a qualitative variable with 2 categories was assessed by Mann-Whitney U test (ie, comparison of the severity of the in vivo reactions, Al particle length, and Al aggregates area between the vaccine and adjuvant-only groups). Association of a nonnormal quantitative variable with a qualitative variable with 3 or more categories was assessed by Kruskal-Wallis test followed by a post hoc Dunn's test (ie, comparisons of the content in Al in the regional lymph nodes among the 3 groups).[5]

Data were analyzed using IBM SPSS 19.0 for Windows (IBM Corp, Armonk, NY, USA). A P value <.05 was considered statistically significant.

Results

In Vivo Studies

In vivo assessment of local reactions is shown in Suppl. Fig. S1. Injection-site nodules were palpated only in the vaccine and adjuvant-only groups. Local reactions in the vaccine group showed a significantly higher ($P < .001$) degree of severity (cumulative median = 0.79, IQR = 0.59–1.04) when compared with adjuvant-only animals (cumulative median = 0.36, IQR = 0.21–0.50). Peaks of severity were observed in both groups in parallel and were associated with a high Al dose in the immediately previous injection. In general, only 1 nodule was palpated per animal, and most of the liquefactive and fistula-forming nodules were observed in the vaccine group (data not shown).

Gross and Histopathology

Inspection of the subcutaneous tissue after the removal of the adipose panniculus revealed the presence of nodules, although only in the vaccine and adjuvant-only groups (Fig. 2). All (26/26; 100%) lambs of the vaccine group and most (24/26, 92.3%) of the adjuvant-only animals presented nodules, whereas the control group (0/26; 0%) did not (Table 1). More than half of the adjuvant-only lambs showed 1 or 2 nodules in total, whereas more than 75% of the vaccine animals exhibited 8 nodules or more; the minimum number of nodules recovered in vaccine animals was 3 (Table 1). Remarkably, 7 vaccine lambs (7/26, 26.9%) showed between 13 and 16 nodules in the right flank (Fig. 3). Vaccine-induced nodules were round and conspicuous (Fig. 4), whereas adjuvant-only–induced nodules tended to be plaque-like or at least not as round (Fig. 5). In both groups, nodule size was generally within a range of 0.5 and 2 cm. However, especially in the adjuvant-only group, some nodules were difficult to locate because of their small size (sometimes less than 2 mm). Central caseous necrosis of nodules was grossly observed in 84.6% and in 13.6% of the vaccine and adjuvant-only lambs, respectively (Figs. 6, 7).

The basic histologic features of the injection site nodules and regional lymph nodes were comparable within and between the 2 treated groups, varying only in their intensities (Table 2), while no control animals presented with injection site reactions. In the 2 treated groups, nodules consisted of well-demarcated granulomas mostly composed of voluminous, activated macrophages showing a vacuolated to coarsely granulated cytoplasm (Figs. 8, 9). Multinucleated giant cells, either Langhans or foreign-body type, were observed significantly more often in granulomas from vaccine animals ($P = .010$; Fig. 8, inset). Lymphocyte aggregates were observed at the periphery of granulomas in half of the animals of both groups. Significantly higher degrees of central necrosis ($P = .021$; Fig. 8) and mineralization ($P = .001$) were observed in granulomas of vaccinated lambs, together with a significant presence of neutrophils ($P = .009$). In both groups, scattered within the granulomas, well-defined, straight-bordered, intra- and extracellular, round to elongated (cigarette-shaped) eosinophilic crystalloid bodies of approximately 100–200 μm were observed. These bodies were significantly overrepresented in adjuvant-only granulomas ($P < .001$; Fig. 9). The prescapular lymph nodes of vaccine and adjuvant-only lambs showed significant cortical hyperplasia ($P < .001$) and significant presence of clusters of voluminous, foamy to granulated macrophages ($P < .001$; Fig. 10).

Using lumogallion staining, a granular, intense intracytoplasmic orange fluorescence was observed in macrophages from granulomas and lymph nodes from both vaccine and adjuvant-only groups (Fig. 11). Remarkably, the eosinophilic crystalloid bodies observed with hematoxylin and eosin showed the most intense orange fluorescence (Fig. 12). Fluorescence of similar characteristics was not observed in tissues from control lambs.

Table 2. Histologic Lesions in Subcutaneous Granulomas and Lymph Nodes in Lambs Injected Subcutaneously With Phosphate-Buffered Saline (Control), Adjuvant-Only or Vaccines.[a]

Granulomas	Scoring	Control	Adjuvant ($n = 23$)	Vaccine ($n = 24$)	*P*
Voluminous macrophages	0	NA	0 (0)	0 (0)	.232[LR]
	1		0 (0)	1 (4.2)	
	2		5 (21.7)	2 (8.3)	
	3		18 (78.3)	21 (87.5)	
Multinucleated giant cells	+	NA	15 (65.2)	23 (95.8)	**.010**[F]
	–		8 (34.8)	1 (4.2)	
Lymphocytes	+	NA	12 (52.2)	13 (54.2)	>.999[F]
	–		11 (47.8)	11 (45.8)	
Tertiary lymphoid tissue	+	NA	2 (8.7)	3 (12.5)	>.999[F]
	–		21 (91.3)	21 (87.5)	
Neutrophils	+	NA	7 (30.4)	17 (70.8)	**.009**[F]
	–		16 (69.6)	7 (29.2)	
Necrosis	0	NA	14 (60.9)	7 (29.2)	**.021**[LR]
	1		4 (17.4)	2 (8.3)	
	2		2 (8.7)	2 (8.3)	
	3		3 (13.0)	13 (54.2)	
Mineralization	0	NA	21 (91.3)	11 (45.8)	**.001**[LR]
	1		2 (8.7)	3 (12.5)	
	2		0 (0)	5 (20.8)	
	3		0 (0)	5 (20.8)	
External fibrosis (capsule)	+	NA	20 (87.0)	24 (100)	.109[F]
	–		3 (13.0)	0 (0)	
Internal fibrosis	+	NA	21 (91.3)	17 (70.8)	.137[F]
	–		2 (8.7)	7 (29.2)	
Internal hemorrhages	+	NA	4 (17.4)	5 (20.8)	>.999[F]
	–		19 (82.6)	19 (79.2)	
External hemorrhages	+	NA	1 (4.3)	2 (8.3)	>.999[F]
	–		22 (95.7)	22 (91.7)	
Internal blood vessels	+	NA	23 (100)	24 (100)	—
	–		0 (0)	0 (0)	
Eosinophilic crystalloid bodies	0	NA	4 (17.4)	19 (79.2)	**<.001**[LR]
	1		4 (17.4)	2 (8.3)	
	2		8 (34.8)	2 (8.3)	
	3		7 (30.4)	1 (4.2)	

Lymph Nodes		Control ($n = 26$)	Adjuvant ($n = 24$)	Vaccine ($n = 26$)	*P*
Cortical hyperplasia[b]	0	1 (3.8)	0 (0)	0 (0)	**<.001**[LR]
	1	9 (34.6)	2 (8.3)	1 (3.8)	
	2	15 (57.7)	10 (41.7)	10 (38.5)	
	3	1 (3.8)	12 (50.0)	15 (57.7)	
Prominent germinal centers	0	0 (0)	0 (0)	0 (0)	.060[χ^2]
	1	9 (34.6)	2 (8.3)	4 (15.4)	
	2	12 (46.2)	11 (45.8)	9 (34.6)	
	3	5 (19.2)	11 (45.8)	13 (50.0)	
Aggregates of voluminous macrophages[b]	+	3 (11.5)	22 (91.7)	22 (84.6)	**<.001**[χ^2]
	–	23 (88.5)	2 (8.3)	4 (15.4)	

Abbreviations: NA, not applicable; LR, likelihood ratio; F, Fisher's exact test; χ^2, Pearson's chi-square test; +, presence; –, absence.

[a] The data show the number (and percentage) of animals with each lesion.

[b] Significant difference refers to comparing vaccine/adjuvant-only groups with control group.

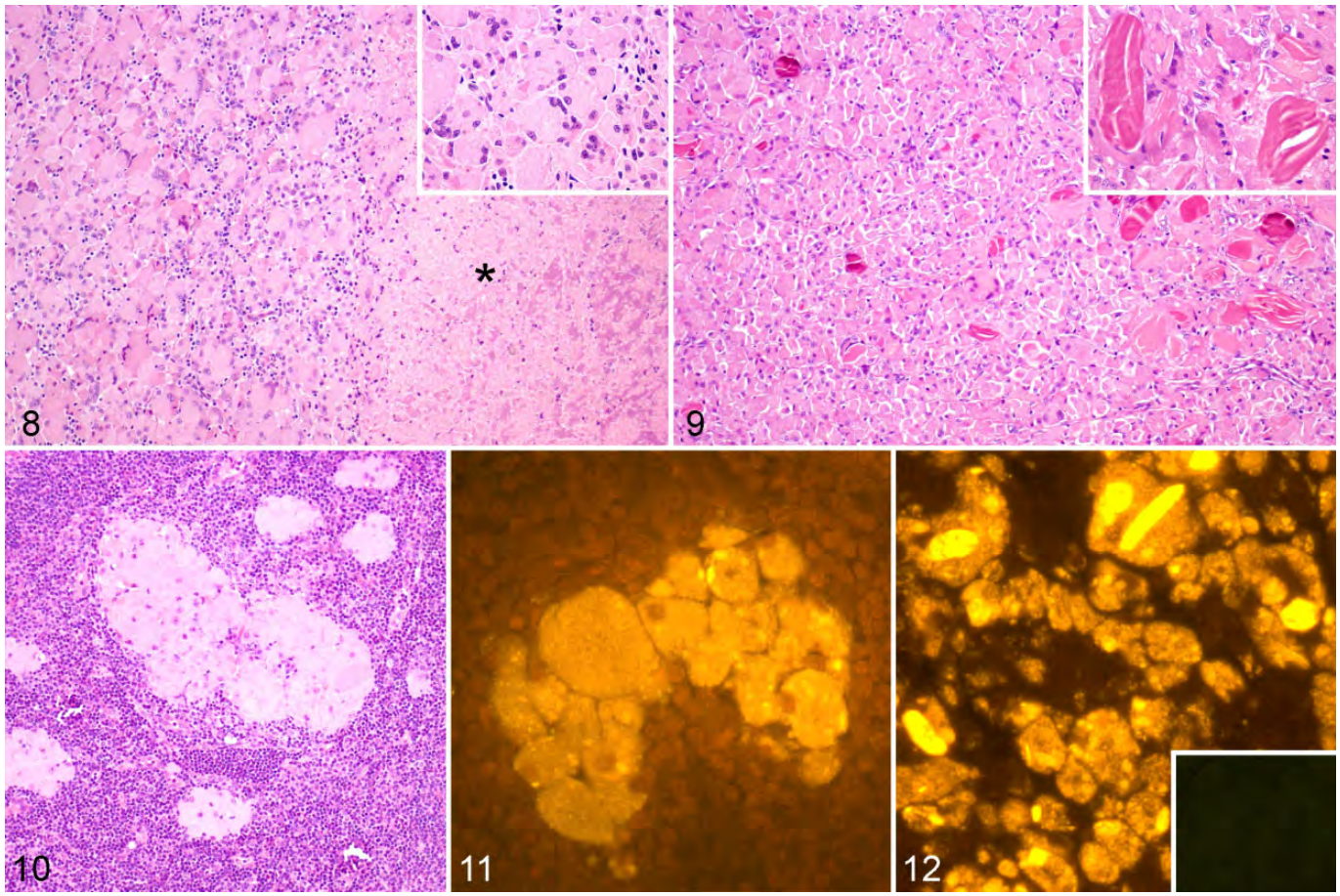

Figures 8–9. Injection site granulomas. Lambs injected subcutaneously with vaccine or adjuvant-only. **Figure 8.** Vaccine group. Dense aggregates of epithelioid macrophages and multinucleated giant cells and a regionally extensive area of necrosis (asterisk). *Inset*: multinucleated giant cells contain foamy cytoplasm. Hematoxylin and eosin (HE). **Figure 9.** Adjuvant-only group. Aggregates of epithelioid macrophages with few multinucleated giant cells intermingled with intra- and extracellular eosinophilic crystalloid bodies. *Inset*: Several eosinophilic crystalloid bodies in close relationship with multinucleated giant cells. HE. **Figures 10–11.** Right prescapular lymph nodes. **Figure 10.** Adjuvant-only group. Coalescing aggregates of macrophages. HE. **Figure 11.** Vaccine group. Aggregates of macrophages showing aluminum (Al)–positive fluorescence. Lumogallion. **Figure 12.** Injection site granuloma, adjuvant-only group. Macrophages showing intracytoplasmic Al-positive orange fluorescence with a granular pattern. Eosinophilic crystalloid bodies show strong positive fluorescence. Lumogallion. *Inset*: Absence of autofluorescence in an unstained sequential section.

Electron Microscopy Studies

Macrophages within granulomas contained needle-shaped, electron-dense material (Fig. 13) that formed multiple intracytoplasmic aggregates, often surrounded by a subcellular membrane (phagolysosome; Figs. 14, 15). This membrane showed occasional areas of discontinuity and loss, leading to the presence of free intracytoplasmic spiculated material. The eosinophilic, lumogallion-positive crystalloid bodies showed a dense and uniform aggregation of the same spiculated material (Fig. 16). Independently of the presentation and location, this needle-shaped material was identified as Al by EDS, and other frequently identified elements were carbon, oxygen, lead, copper, and osmium (Fig. 17). EDS measurements performed in nuclei were always negative for Al. Al particles in granulomas were significantly longer ($P < .001$) in the vaccine group (median = 121.24 nm, IQR = 98.30–170.60) than particles in the adjuvant-only group (median = 69.47 nm, IQR = 53.53–87.62; Fig. 18). The area of aggregates was similar in both groups (vaccine: median = 1.71 μm^2, IQR = 0.84–3.10; adjuvant-only: median = 1.80 μm^2, IQR = 1.19–2.80; Fig. 19). Finally, macrophages in both groups showed 1 or more of the following degenerative changes: swollen rough endoplasmic reticulum with prominent ribosomes, swollen mitochondria with disorganization of cristae, intracytoplasmic myelin figures, nuclear membrane blebs, and indentations and margination of heterochromatin.

Microbiology

All 26 granulomas and the 14 injection site areas from control lambs were negative for bacteriological cultures, and no bacterial forms were observed with Gram staining.

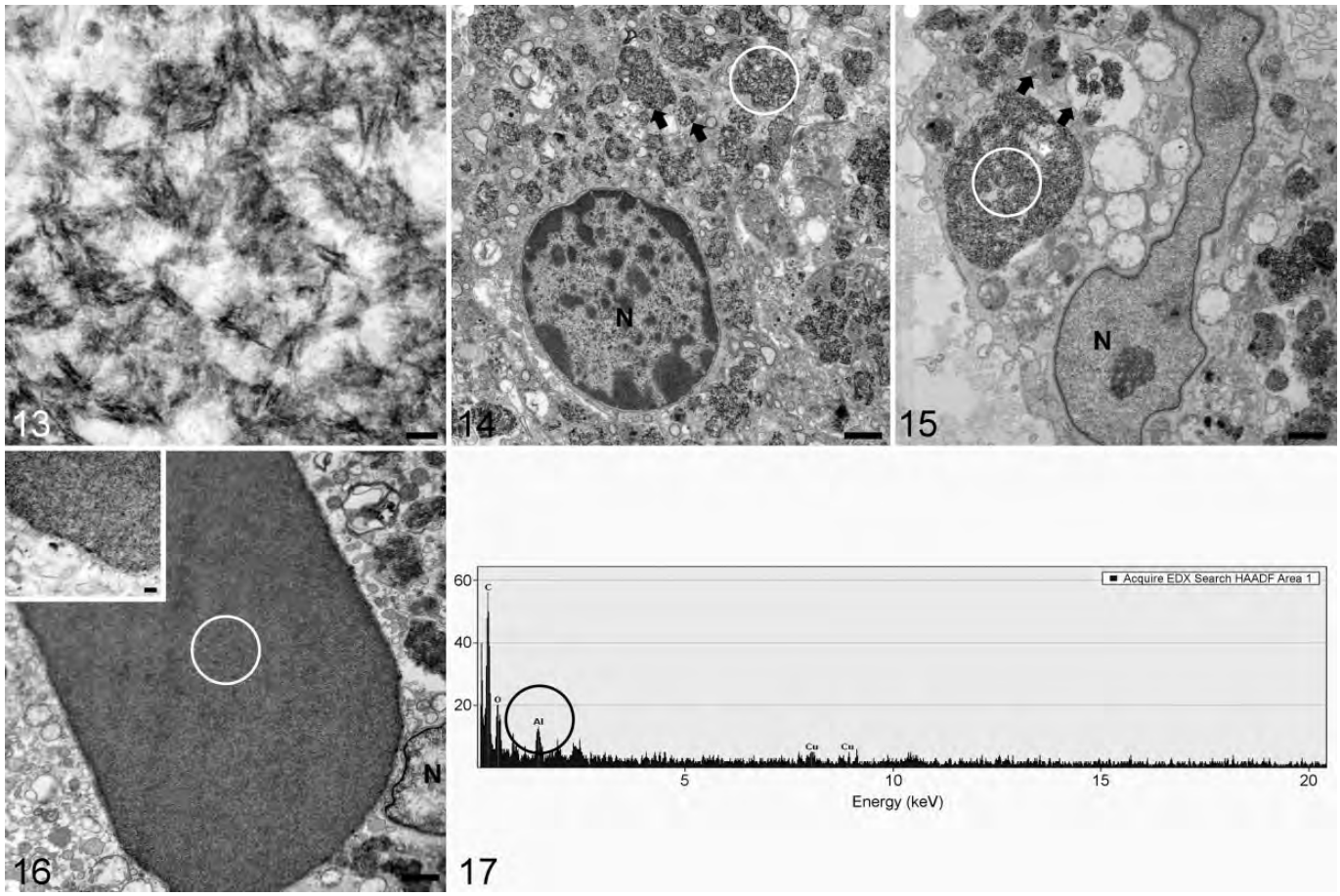

Figures 13–17. Injection site granulomas, lambs injected with vaccine or adjuvant. Scanning transmission electron microscopy and energy-dispersive X-ray spectroscopy (EDS). White circles in the electron micrographs show areas of EDS measurements. **Figure 13.** Vaccine group. Long and prominent electron-dense spiculated particles, identified as aluminum (Al). Bar = 100 nm. **Figure 14.** Vaccine group. Macrophage containing cytoplasmic vesicles (arrows) containing the spiculated electron-dense material identified as Al. Nuclear condensation and peripheralization of heterochromatin. N: nucleus. Bar = 1 μm. **Figure 15.** Adjuvant-only group. Aggregates of Al enclosed in different-sized phagolysosomes (arrows) and nuclear elongation. N: nucleus. Bar = 1 μm. **Figure 16.** Adjuvant-only group. Large and straight-bordered aggregate of densely packed material, which corresponds to the eosinophilic crystalloid bodies observed by hematoxylin-eosin. These aggregates show electron-dense borders. N: nucleus. Bar = 1 μm. *Inset*: Higher magnification of the aggregate border. Bar = 200 nm. **Figure 17.** Representative EDS graph. The spiculated electron-dense material and the crystalloid bodies (indicated in white circles in Figs. 14, 15, and 16) were always identified as Al (peak indicated by a black circle).

Aluminum Content in Lymph Nodes

The content of Al in lymph nodes is detailed in Table 3. The vaccine group contained significantly higher values than the other 2 groups ($P < .001$), and the content of Al in the adjuvant-only animals was also significantly higher than in the control ($P < .001$).

Discussion

This is the first comprehensive description of the morphology of persistent granulomas in sheep following injection with either vaccines containing Al-based adjuvants or the Al-based adjuvant alone. Al was unequivocally identified by different methods both in granulomas and lymph nodes, with higher lesion severity in granulomas from vaccinated lambs. The ultrastructure of the granulomas varied according to whether Al was administered as a vaccine preparation or simply as an adjuvant. The translocation of Al from the injection site to the lymph node was demonstrated for the first time in a large animal model.

This experiment was planned to study the lesions caused by the administration of Al adjuvant-containing products, independent of the identification of individual injections, the exact age of the granuloma, or the role of specific vaccine antigens, as evaluated in other studies.[39] Our results showed that granuloma was the only type of local reaction produced by these injections, differing only in shape, persistency, and histopathologic aspects. Lambs in this experiment were sourced from 4 different flocks. However, in vivo measurements and observations of gross and microscopic changes were similar, irrespective of flock, breed, or management conditions. Therefore, these observations are combined as 3 experimental groups.

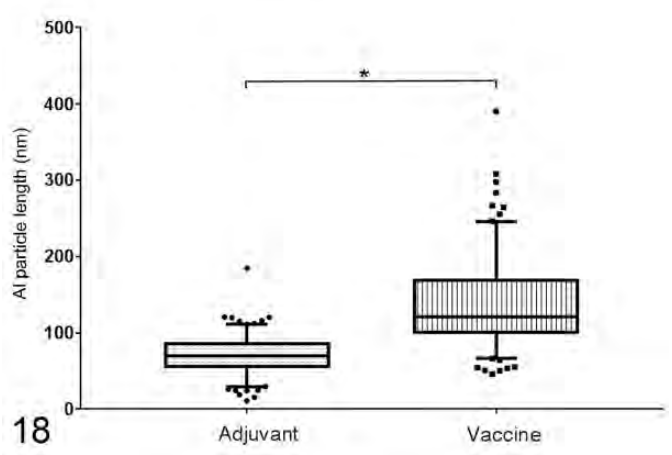

Figure 18. Length of the aluminum (Al) particles in granuloma macrophages. Boxes represent the interquartile range, and horizontal lines inside the boxes represent the median values. Whisker bars represent the variability of the data outside the interquartile range. Points and squares represent the outlier measurements in each group. Vaccine granulomas have significantly longer aluminum particles than adjuvant-only granulomas. *$P < .001$, Mann-Whitney *U* test.

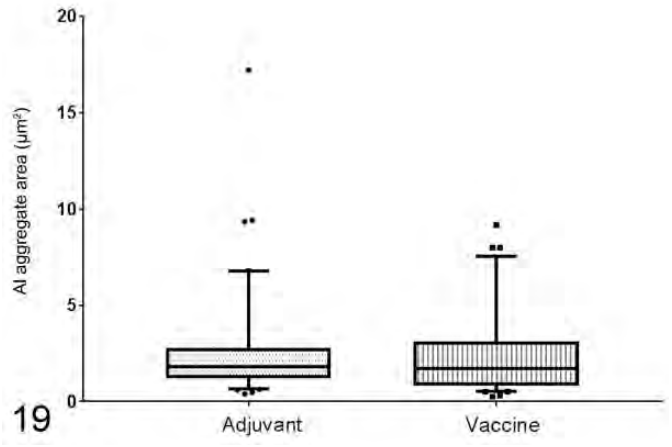

Figure 19. Area of aluminum (Al) aggregates in granuloma macrophages. Boxes represent the interquartile range, and horizontal lines inside the boxes represent the median values. Whisker bars represent the variability of the data outside the interquartile range. Points and squares represent the outlier measurements in each group. Vaccine and adjuvant-only granulomas show a similar aggregate area. *$P <$ NS, Mann-Whitney *U* test.

Gross pathology data demonstrated that injection site granulomas were much more numerous than was noticed by in vivo examination. In sheep, these reactions are reported to disappear with time, although it is not known exactly how long this takes.[33] The gross data underline that the development of granulomas in both treated groups was very common and was a universal fact in the vaccine animals. More than 75% of vaccine animals demonstrated at least 8 granulomas, indicating more frequent development or persistence of granulomas induced by vaccines. Assuming that each granuloma corresponded to a different single injection, the postmortem detection of granulomas in all injection sites would indicate that they may persist for at least 15 months, the duration of the current experiment. This persistence might reflect a low capacity, perhaps genetic, for clearing Al from the injection site in certain lambs, as has also been postulated in humans with specific human leukocyte antigen polymorphisms.[14] Granulomas induced in adjuvant-only animals showed a lower persistency, which might indicate a quicker clearance of Al, perhaps due to a less severe immune reaction from the lack of antigen and/or different Al particle conformation.

Histologically, the reactions observed were interpreted as immune-mediated granulomas (ie, they are induced by persistent immunostimulating agents).[24] In the vaccine group, there were more frequent and extensive necrotic centers, which might be due to the presence of antigens, different Al particle conformations, or a combination of both. It is known that Al particle size can increase in the presence of antigens,[35] and indeed our results point to a higher particle size in vaccine granulomas. Al particles have been linked to phagolysosome membrane disruption and release of Al into the cytoplasm, leading to cell death by activating the cathepsin-mediated necrosis pathway.[20] Indeed, a relationship between particle size and the immunostimulation capability of different adjuvants has been postulated.[32,41] Therefore, a different particle conformation due to the interaction with antigen may induce an increased immune stimulation, leading to a higher degree of tissue necrosis in vaccine granulomas. More accurate methods[21,35] should be employed to determine real particle size, as our measurements are only 2-dimensional estimations of particle length for comparison purposes. We describe for the first time large dense Al aggregates in the form of pale crystalloid eosinophilic bodies with straight borders within the granulomas, the number of which was significantly increased in the adjuvant-only group. The reason for formation of these crystalloid bodies remains obscure, and further research is needed to clarify their role in the genesis of the granulomas and subsequent interactions with the surrounding tissues.

Lumogallion demonstrated excellent performance in granulomas and lymph nodes, giving an Al-selective orange fluorescence[30,31] that is easier to interpret than other stains.[13] This technique has recently been used to reliably identify Al in tissues from rats fed an Al-containing diet.[28] EDS has been previously used to determine the presence of Al in postvaccine granulomas in pigs[38] and humans.[22] The presence of other elements in EDS determinations are explained by the technical processing of the samples: lead and osmium are part of the staining, and copper is in the grid.[38] TH GFAAS has been used to determine Al content in human[29] and animal tissues.[4,28] In our study, this technique demonstrated a significant increase of Al in lymph nodes of vaccine lambs when compared with both adjuvant-only and control animals. Quantitative analyses using TH GFAAS and qualitative imaging using lumogallion demonstrate for the first time in a large animal model that Al is carried in macrophages from the injection site to lymph nodes. In fact,

Table 3. Aluminum (Al) Content in the Right Prescapular Lymph Node of Lambs Injected Subcutaneously With Phosphate-Buffered Saline (Control), Adjuvant-Only or Vaccine.[a]

	Control	Adjuvant	Vaccine	P*
Al (μg/g)	0.96[a] (0.68 -1.39)	2.53[b] (1.99-7.19)	82.65[c] (20.62-682.27)	<.001

[a] The data show the median and range. Different superscripts (a, b, c) indicate statistically significant differences between the groups.
*Kruskall-Wallis test with post hoc Dunn test.

egress of mycobacteria-infected macrophages from granulomas is a well-described mechanism,[6] and translocation of metals to lymph nodes has recently been reported in a case of a dog with hip-implant–associated metallosis[8] and also in humans with subcutaneous tattoos that carry a variety of metals, including Al.[34] The Al translocation observed in this work might suggest a systemic distribution throughout the body, as demonstrated in mice[23] or rabbits.[11] In our animals, Al-containing macrophages tended to form aggregates in the lymph nodes, as has been similarly observed in mice.[18,23] Some control lambs showed rare, similar but smaller macrophage aggregates, negative to lumogallion staining, in the draining lymph node (Table 2) that might simply indicate the drainage of other, nonrelated lipidic phagocytic debris to the lymph node.[10]

This experiment was part of a comprehensive study to improve understanding of the ovine ASIA syndrome, and it has been successful in reproducing some, but not all, of its most remarkable changes. Vaccine and adjuvant-only groups demonstrated significant changes in the interindividual and intragroup interaction patterns (ie, increase in wool biting and restlessness) as the cumulative number of injections increased. These findings coincide with previous observations on the ovine ASIA syndrome.[27] Treatment groups also showed higher levels of stress biomarkers, and the clinicopathological picture as a whole showed few significant differences between these groups. These results will be published in detail elsewhere.

Conclusion

In sheep, persistent subcutaneous granuloma formation is a universal reaction to the injection of Al either in commercial vaccines or simply as Al-based adjuvants. We show that Al is subsequently transported from the injection site to the lymph nodes. This transport was far more pronounced in the commercial vaccine preparations, which suggests that the animal handles Al differently depending upon its presentation at injection sites. Further research is needed to study the putative role of this tissue reaction in the development of the previously described ovine ASIA syndrome.

Acknowledgements

We deeply thank all veterinarians and farmers who contributed to the development of the experiment. We are indebted to Prof. Jesús Santamaría (INA, University of Zaragoza) for his help on the use of electron microscopy facilities. We thank all the undergraduate and postgraduate students of the Ruminants Clinic Service (SCRUM) of the University of the Zaragoza for their help. Rosario Puyó and Santiago Becerra are acknowledged for their technical support. We would like to acknowledge the use of Servicio General de Apoyo a la Investigación (SAI), Universidad de Zaragoza.

Declaration of Conflicting Interests

The authors declared no potential conflicts of interest with respect to the research, authorship, and/or publication of this article.

Funding

This work was funded by grants from the Spanish Ministry of Economy and Industry (AGL2013-49137-C3-1-R and AGL2013-49137-C3-2-R). J. Asín is a PhD student funded by the Spanish Ministry of Education, Culture and Sports. R. Reina is supported by a "Ramón y Cajal" contract from the Spanish Ministry of Economy, Industry and Competitiveness.

ORCID iD

Matthew Mold http://orcid.org/0000-0002-4616-6204
Lluís Luján http://orcid.org/0000-0002-2053-9842

References

1. Burakova Y, Madera R, McVey S, et al. Adjuvants for animal vaccines. *Viral Immunol*. 2018;**31**(1):11–22.
2. Campos AC, Azevedo EO, Alcântara MDB, et al. Efficiency of inactive vaccines against contagious agalactia in Brazil. *Arq Bras Med Vet Zoot*. 2013;**65**(5):1394–1402.
3. Chong H, Brady K, Metze D, et al. Persistent nodules at injection sites (aluminium granuloma)—clinicopathological study of 14 cases with a diverse range of histological reaction patterns. *Histopathology*. 2006;**48**(2):182–188.
4. Crepeaux G, Eidi H, David MO, et al. Non-linear dose-response of aluminium hydroxide adjuvant particles: selective low dose neurotoxicity. *Toxicology*. 2017;**375**:48–57.
5. Daniel WW, Cross CL. *Biostatistics: A Foundation for Analysis in the Health Sciences*. 10th ed. Singapore: John Wiley & Sons; 2013.
6. Davis JM, Ramakrishnan L. The role of the granuloma in expansion and dissemination of early tuberculous infection. *Cell*. 2009;**136**(1):37–49.
7. de Diego AC, Sanchez-Cordon PJ, Sanchez-Vizcaino JM. Bluetongue in Spain: from the first outbreak to 2012. *Transbound Emerg Dis*. 2014;**61**(6):e1–e11.
8. DiVincenzo MJ, Frydman GH, Kowaleski MP, et al. Metallosis in a dog as a long-term complication following total hip arthroplasty. *Vet Pathol*. 2017;**54**(5):828–831.
9. Eisenbarth SC, Colegio OR, O'Connor W, et al. Crucial role for the Nalp3 inflammasome in the immunostimulatory properties of aluminium adjuvants. *Nature*. 2008;**453**(7198):1122–1126.
10. Elmore SA. Histopathology of the lymph nodes. *Toxicol Pathol*. 2006;**34**(5):425–454.
11. Flarend RE, Hem SL, White JL, et al. In vivo absorption of aluminium-containing vaccine adjuvants using ^{26}Al. *Vaccine*. 1997;**15**(12–13):1314–1318.

12. Gonzalez JM, Figueras L, Ortega ME, et al. Possible adverse reactions in sheep after vaccination with inactivated BTV vaccines. *Vet Rec*. 2010;**166**(24): 757–758.
13. Guillard O, Fauconneau B, Pineau A, et al. Aluminium overload after 5 years in skin biopsy following post-vaccination with subcutaneous pseudolymphoma. *J Trace Elem Med Biol*. 2012;**26**(4):291–293.
14. Guis S, Pellissier JF, Nicoli F, et al. HLA-DRB1*01 and macrophagic myofasciitis. *Arthritis Rheum*. 2002;**46**(9):2535–2537.
15. Hargis AN, Myers S. The integument. In: Zachary JF, ed. *Pathologic Basis of Veterinary Disease*. 6th ed. St Louis, MO: Elsevier; 2017:1065.
16. Hartmann K, Day MJ, Thiry E, et al. Feline injection-site sarcoma: ABCD guidelines on prevention and management. *J Feline Med Surg*. 2015;**17**(7): 606–613.
17. Hendrick MJ, Goldschmidt MH, Shofer FS, et al. Postvaccinal sarcomas in the cat: epidemiology and electron probe microanalytical identification of aluminum. *Cancer Res*. 1992;**52**(19):5391–5394.
18. HogenEsch H, Dunham A, Burlet E, et al. Preclinical safety study of a recombinant *Streptococcus pyogenes* vaccine formulated with aluminum adjuvant. *J Appl Toxicol*. 2017;**37**(2):222–230.
19. House E, Esiri M, Forster G, et al. Aluminium, iron and copper in human brain tissues donated to the medical research council's cognitive function and ageing study. *Metallomics*. 2012;**4**(1):56–65.
20. Jacobson LS, Lima H Jr, Goldberg MF, et al. Cathepsin-mediated necrosis controls the adaptive immune response by Th2 (T helper type 2)-associated adjuvants. *J Biol Chem*. 2013;**288**(11):7481–7491.
21. Johnston CT, Wang SL, Hem SL. Measuring the surface area of aluminum hydroxide adjuvant. *J Pharm Sci*. 2002;**91**(7):1702–1706.
22. Kalil RK, Monteiro A Jr, Lima MI, et al. Macrophagic myofasciitis in childhood: the role of scanning electron microscopy/energy-dispersive spectroscopy for diagnosis. *Ultrastruct Pathol*. 2007;**31**(1):45–50.
23. Khan Z, Combadiere C, Authier FJ, et al. Slow CCL2-dependent translocation of biopersistent particles from muscle to brain. *BMC Med*. 2013;**11**:99.
24. Kumar V, Abbas AK, Aster JC. Inflammation and repair. In: Kumar V, Abbas AK, Aster JC, eds. *Robbins and Cotrand Pathologic Basis of Disease*. 9th ed. Philadelphia, PA: Elsevier; 2016:69–113.
25. Lacasta D, Ferrer LM, Ramos JJ, et al. Vaccination schedules in small ruminant farms. *Vet Microbiol*. 2015;**181**(1–2):34–46.
26. Lindblad EB. Aluminium compounds for use in vaccines. *Immunol Cell Biol*. 2004;**82**(5):497–505.
27. Luján L, Perez M, Salazar E, et al. Autoimmune/autoinflammatory syndrome induced by adjuvants (ASIA syndrome) in commercial sheep. *Immunol Res*. 2013;**56**(2–3):317–324.
28. Martinez CS, Escobar AG, Uranga-Ocio JA, et al. Aluminum exposure for 60 days at human dietary levels impairs spermatogenesis and sperm quality in rats. *Reprod Toxicol*. 2017;**73**(Suppl C):128–141.
29. Mirza A, King A, Troakes C, et al. Aluminium in brain tissue in familial Alzheimer's disease. *J Trace Elem Med Biol* 2017;**40**:30–36.
30. Mirza A, King A, Troakes C, et al. The identification of aluminum in human brain tissue using lumogallion and fluorescence microscopy. *J Alzheimers Dis*. 2016;**54**(4):1333–1338.
31. Mold M, Eriksson H, Siesjo P, et al. Unequivocal identification of intracellular aluminium adjuvant in a monocytic THP-1 cell line. *Sci Rep*. 2014;**4**:6287.
32. Oyewumi MO, Kumar A, Cui Z. Nano-microparticles as immune adjuvants: correlating particle sizes and the resultant immune responses. *Expert Rev Vaccines*. 2010;**9**(9):1095–1107.
33. Ross AD, Titterington DM. Injection site lesions of footrot vaccines in sheep. *N Z Vet J*. 1984;**32**(1–2):6–8.
34. Schreiver I, Hesse B, Seim C, et al. Synchrotron-based nu-XRF mapping and mu-FTIR microscopy enable to look into the fate and effects of tattoo pigments in human skin. *Sci Rep*. 2017;**7**(1):11395.
35. Shardlow E, Mold M, Exley C. From stock bottle to vaccine: elucidating the particle size distributions of aluminum adjuvants using dynamic light scattering. *Front Chem*. 2016;**4**:48.
36. Shoenfeld Y, Agmon-Levin N. 'ASIA'—autoimmune/inflammatory syndrome induced by adjuvants. *J Autoimmun*. 2011;**36**(1):4–8.
37. Spickler AR, Roth JA. Adjuvants in veterinary vaccines: modes of action and adverse effects. *J Vet Intern Med*. 2003;**17**(3):273–281.
38. Valtulini S, Macchi C, Ballanti P, et al. Aluminium hydroxide-induced granulomas in pigs. *Vaccine*. 2005;**23**(30):3999–4004.
39. Verdier F, Burnett R, Michelet-Habchi C, et al. Aluminium assay and evaluation of the local reaction at several time points after intramuscular administration of aluminium containing vaccines in the Cynomolgus monkey. *Vaccine* 2005; **23**(11):1359–1367.
40. Woodward KN, Toon LA. Adverse reactions to vaccines. In: Woodwar KN, ed. *Veterinary Pharmacovigilance: Adverse Reactions to Veterinary Medicinal Products. 1st ed*. West Sussex, UK: Wiley-Blackwell; 2009; 453–475.
41. Xiang SD, Scholzen A, Minigo G, et al. Pathogen recognition and development of particulate vaccines: does size matter? *Methods*. 2006;**40**(1):1–9.